Nanoscale

Iodine Activation: A General Method for Catalytic Enhancement of Thiolate Monolayer-Protected Metal Clusters

Journal:	*Nanoscale*
Manuscript ID	NR-ART-01-2020-000844.R1
Article Type:	Paper
Date Submitted by the Author:	28-Apr-2020
Complete List of Authors:	Sibakoti, Tirtha; University of Louisville, Chemsitry Jasinski, Jacek; Universiyty of Louisville, Conn Center for Renewable Energy Research Nantz, Michael; University of Louisville, Chemistry Zamborini, Francis; University of Louisville, Chemsitry

Iodine Activation: A General Method for Catalytic Enhancement of Thiolate Monolayer-Protected Metal Clusters

Tirtha R. Sibakoti,[a] Jacek B. Jasinski,[b] Michael H. Nantz*[a] and Francis P. Zamborini*[a]

[a]Department of Chemistry and [b]Conn Center for Renewable Energy Research, University of Louisville, Louisville, Kentucky 40292, United States

Abstract

To enhance catalytic activity, the present study details a general approach for partial thiolate ligand removal from monolayer-protected clusters (MPCs) by straightforward in-situ addition of iodine. Two model reactions are examined to illustrate the effects on the catalytic activity of glutathione (SG)-capped Au MPCs serving as a catalyst for the $NaBH_4$ reduction of 4-nitrophenol to 4-aminophenol and SG-capped Pd MPCs serving as a catalyst for the hydrogenation/isomerization of allyl alcohol. Iodine addition promoted partial thiolate ligand removal from both MPCs and improved the catalytic properties, presumably due to greater surface exposure of the metal cores as a result of ligand dissociation. The rate of 4-nitrophenol reduction increased from 0.066 min^{-1} in the absence of I_2 to 0.505 min^{-1} in the presence of 2.0 equivalents I_2 (equivalents based on total ligated glutathione). The reaction of allyl alcohol to produce 1-propanol and propanal was similarly accelerated as indicated by the increase in turnover frequency from 131 to 230 moles products/moles catalyst/h by addition of 0.2 equivalents I_2. In both reactions, as the amount of I_2 added increases the catalyst recyclability decreases due to catalyst instability. Low equivalents of I_2 are optimal when considering both reaction rate and catalyst recyclability.

* Corresponding authors:

email: michael.nantz@louisville.edu f.zamborini@louisville.edu

phone: (502) 852-8069 (502) 852-6550

Introduction

Metal monolayer-protected clusters (MPCs) stabilized by organothiol monolayers have been used broadly as homogeneous and heterogeneous catalysts in numerous organic transformations,[1, 2] including nitro group reduction,[3] alkene isomerization,[4] alkyne hydrogenation,[5, 6] and Suzuki-Miyaura coupling reactions.[7] The great advantage in using metal MPCs is the excellent synthetic control over the metal cluster size and composition, which allows strong control over the metal structural and electronic properties for tuning catalytic activity. The use of a wide variety of thiol-containing capping ligands enables high stability, tuning of the solubility properties, potential molecular gating properties, and the ability to treat these molecular metals as normal chemical reagents, thereby allowing characterization by standard analytical spectroscopic tools of the organic chemist (e.g., nuclear magnetic resonance spectroscopy (NMR), Fourier-transform infrared spectroscopy (FTIR), mass spectrometry (MS), and UV-vis).[8] Additionally, improvements in separation methods have led to syntheses of highly uniform MPCs of one composition, also known as atomically-precise clusters, such as the widely studied $Au_{25}(SR)_{18}$ cluster product.[9, 10] While use of thiol ligands as capping agents affords tremendous synthetic control, they also strongly passivate the metal cluster surface and poison (or inhibit) the catalytic properties. As a result, there is much interest in developing new ligand systems or incorporating strategies to increase MPC catalytic activity without sacrificing stability. This is a tremendous challenge as the two — ligand-imparted stability vs. ligand-diminished activity — work directly against each other.

One main strategy for balancing the stabilizing properties of a given ligand while increasing reactant access to the metal core, essential for catalytic activity to occur,[11] is the use of lower coverage thiol ligands, such as those derived from Bunte salts,[12, 13] or branched, bulky thiol-

containing ligands, so as to decrease ligand surface density.[14] Bhama *et al.* recently demonstrated the use of branched, water-soluble glutathione (SG)-capped Pd MPCs, which catalyzed the hydrogenation/isomerization of allyl alcohol with a turnover frequency (TOF) roughly 5 times greater than linear chain hexanethiol-stabilized Au MPCs.[15] Another common approach is to activate MPCs by post-synthesis ligand removal. Examples of this include electrochemically-induced ligand desorption,[16] UV-ozone ligand decomposition,[17] thermal annealing,[18, 19] and various chemical treatments.[20, 21] These ligand removal strategies are more effective for heterogeneous catalysis applications with solid-supported metal MPCs because some of the ligand-removing approaches require either an electrode surface or gas-phase conditions, otherwise the approach is not controlled and particle growth or other morphological changes quickly diminish the catalytic properties. Our interest in the synthesis of functionalized Au and Pd nanoclusters[22] and their applications in sensing[23] and catalysis[24] have motivated us to consider an alternate method for catalytic activation.

In their seminal study on organothiolate Au MPCs, Templeton *et al*.[25] showed that reaction with iodine results in decomposition of the MPCs with concomitant formation of desorbed disulfide species. The use of I_2 in this manner is often used as a means for confirming the identity of ligated thiols on MPCs by NMR. Generally, a few crystals of I_2 are added to an NMR tube containing thiolate-protected MPCs to 'knock off' the thiol ligand so as to obtain a ^{1}H NMR spectrum of the resultant, corresponding disulfide. Iodine-induced disulfide formation has been cleverly harnessed by Sun *et al*. in their report on the synthesis of hollow spheres comprised of polycyclodextrin.[26] After preparing Au MPCs coated with a monolayer of thiolated β-cyclodextrin molecules, the ligated thiols were cross-linked by addition of I_2 in aqueous KI to afford a polycyclodextrin structure comprising a hollow sphere, formed on oxidation and

dissolution of the Au core by the excess iodide. In another example, Kim *et al.* cleaved thiol polymers ligated to Au nanoparticles (NPs) by addition of I_2 to determine the molecular weight and polydispersity of the released polymers after disulfide reduction using $NaBH_4$.[27] These examples of thiol ligand removal from the surface of Au nanostructures have motivated us to examine reaction with I_2 as a means to enhance the catalytic activity of organothiolate metal MPCs.

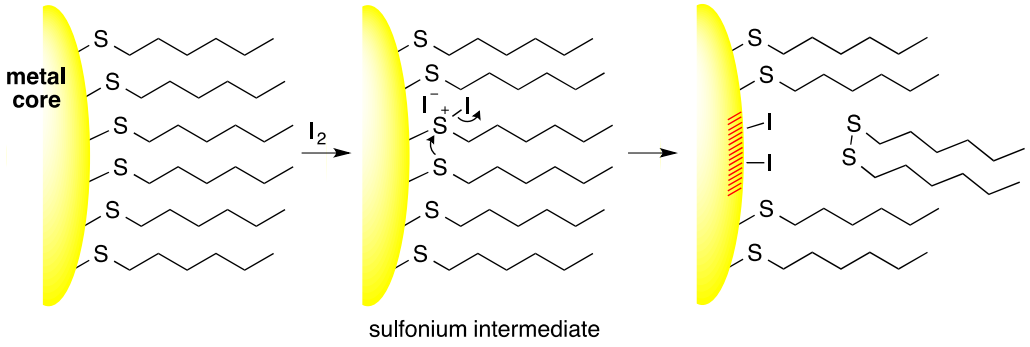

Scheme 1. Iodine activation at the surface of a thiolate-coated metal cluster. We postulate neighboring thiolate displacement of iodide from a sulfonium ion intermediate results in disulfide formation and ligand dissociation, making the metal surface accessible for substrate binding (shaded area). Iodide can presumably adsorb to the metal surface or dissolve into solution.

We hypothesized that treatment of a thiol-capped MPC catalyst with a small quantity of I_2 would lead to well-controlled partial ligand removal by disulfide formation in-situ (Scheme 1), resulting in partial exposure of the metal surface to substrates for enhanced binding and reactivity. To test the I_2-activation concept, we examined two model reactions (Scheme 2): Au MPC-catalyzed reduction of 4-nitrophenol (4-NP) to 4-aminophenol (4-AP) by sodium borohydride,[28] a reaction that has been well-studied using a variety of free or immobilized nanoparticles/clusters as catalysts,[29] and the Pd MPC-catalyzed hydrogenation/isomerization of allyl alcohol in the presence of H_2 to afford propanal and 1-propanol as the isomerized and hydrogenated products,

respectively.[30, 31] We report herein our findings on the influence of I_2 on both the rate of the reaction/turnover frequency (TOF) and recyclability using SG-stabilized Au and Pd MPCs as catalysts.

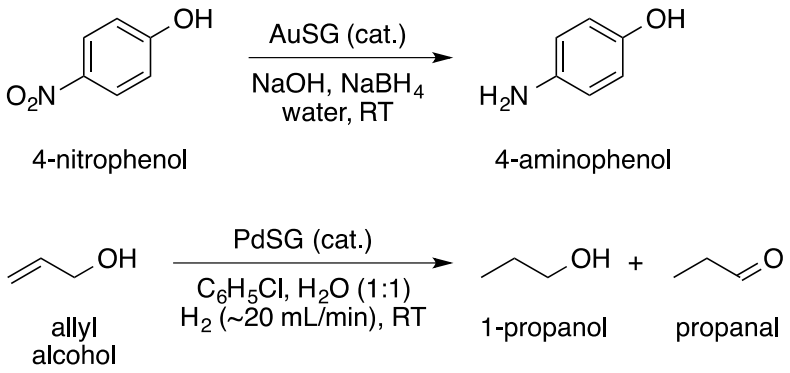

Scheme 2. Model reduction and hydrogenation/isomerization reactions subjected to catalyst activation using I_2.

Experimental Section

Materials. $HAuCl_4 \cdot 3H_2O$ was synthesized from metallic bulk gold according to the literature.[32] Sodium borohydride (≥98.5% reagent grade), 4-nitrophenol solution (10 mM in THF), L-glutathione reduced (≥98.0%), iodine (≥99.8%), ACS grade methanol, tetrahydrofuran, ethanol, acetone, 2-propanol (99.9%), allyl alcohol (99%), propionaldehyde (99%), potassium tetrachloropalladate(II) (99%), chlorobenzene (98%), and sodium hydroxide were purchased and used as received. Deuterium oxide (D_2O) and methanol-d_4 (CD_3OD) were purchased from Cambridge Isotope Laboratories. A N_2 and H_2 gas cylinder were supplied by Welders Supply. Indium-tin-oxide-coated glass slides (Delta Technologies, Ltd.) with a resistivity R_s = 8-12 Ω were used for anodic stripping voltammetry (ASV) measurements. Water was purified using a Barnstead water ultra-purification system (ThermoFisher; R_s = 18.2 MΩ•cm).

Synthesis of AuSG MPCs. Water-soluble glutathione (SG)-functionalized Au MPCs were synthesized using a 3:1 molar ratio of glutathione to $HAuCl_4 \cdot 3H_2O$ as previously described.[33] The synthesis was carried out under a nitrogen atmosphere. Glutathione (120 mg, 0.380 mmol) was added to 400 mL of a methanolic $HAuCl_4 \cdot 3H_2O$ solution (50.1 mg, 0.127 mmol) in a 1-L single-necked round-bottom flask. The bright yellow $HAuCl_4$ solution turned into a light-yellow solution upon addition of glutathione and the mixture was purged with N_2 for 1 hour. The reaction mixture was cooled to 0 °C using an ice bath and stirred for 30 minutes to form a cloudy white color indicative of an Au(I)-SG complex. To the reaction mixture was rapidly added a freshly prepared, chilled methanolic $NaBH_4$ solution (125 mL of a 0.21 M solution, 0.0264 mol) to yield a black reaction mixture indicating the formation of Au SG MPCs. The flow of N_2 was stopped at this stage. The reaction mixture was stirred at room temperature for 12 hours whereupon the Au MPCs precipitated and were isolated by discarding the supernatant. The precipitate was dissolved in nanopure H_2O (10 mL) and an excess amount of methanol (60 mL) was added to again precipitate the clusters, which were collected via centrifugation. The same process was repeated once more to remove any remaining unbound glutathione as well as diborane or disulfide species that may have formed during the synthesis. Finally, the Au SG MPCs were air-dried to afford AuSG MPCs (42.0 mg) as a black powder.

Synthesis of PdSG MPCs. Water-soluble glutathione (SG)-capped Pd MPCs were synthesized using a 0.35:1 molar ratio of glutathione to K_2PdCl_4, as previously described.[14] The synthesis was carried out under a N_2 atmosphere in a three-necked round bottom flask. First, K_2PdCl_4 (0.205 g, 0.628 mmol) was dissolved in nanopure water (20 mL) and the resultant solution was purged with N_2 for 1 hour. Reduced-L-glutathione (0.066 g, 0.221 mmol) was dissolved in nanopure water (10 mL) and purged with N_2 for 1 hour. These two solutions were then

combined at room temperature and stirred under N_2 atmosphere until $PdCl_4^{2-}$ formed a complex with glutathione, as indicated by the change in color from yellow to wine red (*ca.* 5 min). The reaction mixture was further stirred for 1 hour and then cooled to 0 °C using an ice-bath. A fresh aqueous solution of $NaBH_4$ (0.232 g, 6.12 mmol) in nanopure water (10 mL) was purged with N_2 for 1 hour before rapidly adding to the reaction mixture with vigorous stirring to result in an immediate color change from wine red to black. The solution was further stirred for 6 h at room temperature before an equal volume of methanol (40 mL) was added. The resultant suspension was stirred 15 minutes and then centrifuged 15 minutes to precipitate the MPCs. The supernatant was discarded and the precipitated MPCs were collected by dissolving in nanopure water to aid the transfer into a round bottom flask. The water was then removed by using a rotary evaporator. The obtained black MPCs were suspended in methanol (100 mL) overnight and collected by vacuum filtration using a glass fritted Büchner funnel. The MPCs were thoroughly washed with methanol (2x), ethanol (2x), acetone (2x), and then air-dried to afford PdSG MPCs (112 mg) as a black powder.

4-Nitrophenol reduction. A solution of 4-nitrophenol (4-NP) (0.5 mL of 0.3 mM aq. solution, 0.00015 mmol) was added to nanopure H_2O (4.14 mL; this volume varies based on whether an I_2 solution is added at a later stage). Then, NaOH (60 µL of 20 mM aq. solution, 0.0012 mmol, 8 eq.) was added to give a bright yellow solution and followed by addition of $NaBH_4$ (150 µL of 0.1 M aq. solution, 0.015 mmol, 100 eq). Finally, a solution of AuSG MPCs (150 µL of a stock solution, prepared by dissolving 2.0 mg AuSG MPCs in 20 mL nanopure water, 5.1×10^{-5} mmol Au, 0.34 eq of Au) was added to the reaction mixture to obtain a total reaction mixture volume of 5.0 mL. The reaction mixture was let sit at room temperature for 30 seconds before removing an aliquot (3 mL) for UV absorption measurements in a clean quartz cuvette, recording the

absorption spectrum between 250 to 750 nm. Absorption measurements were taken every 1 min or longer as required.

For additions of I_2 to the reaction mixture, a methanolic stock solution of I_2 (0.0539 mM) was first prepared and the corresponding I_2 equivalents (75 μL of stock solution = 0.25 equivalents, based on glutathiolate calculated using an organic composition determined for the AuSG MPCs by TGA of 33%) were then added to the reaction vial. In each reaction examined, the final total reaction volume was maintained at 5.0 mL by adjusting the amount of water used in the first step.

To assess the recyclability of the Au SG MPCs, fresh 4-NP (0.015 mL of 10 mM solution in THF, 0.00015 mmol) was added to the final reduction mixture of the first cycle in the cuvette within 2 minutes after the completed 4-NP reduction. UV-vis measurements then were resumed until the added 4-NP was completely reduced. This cycle was repeated until the 4-NP absorbance remained unchanged. A product removal approach was used to assess the effect of product accumulation on the recyclability of the catalyst. In this experiment, to a solution of 4-NP (4.8 mL of a 0.0042 M aq. solution, 0.02 mmol) were added successively NaOH (50 μL of 3.2 M aq. solution, 0.16 mmol, 8 eq.), $NaBH_4$ (150 μL of 13.3 M aq. solution, 2.00 mmol, 100 eq), and AuSG MPCs (2.0 mg AuSG MPCs, 6.8 x 10^{-3} mmol Au, 0.34 eq of Au). A methanolic stock solution of I_2 (11.5 mM) was first prepared and the corresponding I_2 equivalents (75 μL of stock solution = 0.5 equivalents), were then added to the reaction mixture. Within a minute, an aliquot (22.5 μL) of the reaction mixture was added into a quartz cuvette and diluted with nanopure water (3 mL) for UV absorption measurement. Upon the completion of first reaction cycle, the products were removed via centrifugation (2-fold THF, 10 mL) for 15 min (3x) and the precipitated AuSG MPCs were immediately reused for the next cycle.

Allyl alcohol hydrogenation/isomerization. The hydrogenation/isomerization reaction was performed by dissolving PdSG MPCs (6.0 mg) in nanopure water (2 mL) in a 10 mL glass vial fitted with a stir bar. To the solution was added chlorobenzene (2 mL) and allyl alcohol (200 μL) to form a biphasic reaction mixture. The reaction mixture was then stirred at 800-1000 rpm at room temperature. Hydrogen gas was purged into the reaction mixture at a flow rate of 20.0 ± 0.5 mL/min through a glass pipette. Stirring was ceased and aliquots (20 μL) were removed from both the aqueous and organic phase at 5 min intervals or as required. MPCs in the aqueous phase aliquot were precipitated by adding THF (40 μL) and then centrifuged at 4000 rpm for 10 min. For additions of I_2 to the reaction mixture, a fresh methanolic stock solution of I_2 (5 mM) was first prepared and the corresponding I_2 equivalents (e.g., 28 μL of 5 mM stock solution = 0.025 equivalents relative to SG ligands) were then added to the reaction vial. For the I_2-catalyzed reactions, the final total reaction volume was kept at 4.0 mL by adjusting the 2.0 mL of water used in the first step.

For recycling experiments, the products were extracted into chlorobenzene (4.0 mL) and the organic layer was then removed. This process was repeated two more times to ensure full removal of the products. UV-Vis and GC analyses of the aqueous layer were performed to confirm that no products remained in the aqueous phase. For each consecutive cycle, fresh substrate (200 μL) and chlorobenzene (2 mL) were added. To compensate the volume loss, nano-pure water also was added as required in the consecutive cycles. The cycles were repeated until the reaction required more than 60 minutes to complete.

Electron microscopy measurements. Transmission electron microscopy (TEM) images were obtained using a FEI Tecnai F20 FEG operated in TEM mode with an acceleration voltage of 200 kV. TEM data analysis was carried out using digital micrograph software (version 3.11.0)

and ImageJ software for particles size analysis. TEM samples of water-soluble glutathione-capped Au and Pd MPCs were prepared by dissolving in water (0.5 mg/1 mL) and then drop casting the aqueous solution (10 μL) on a 400 mesh Formvar/carbon-coated copper grid, letting it air-dry for at least 4 hours. Scanning electron microscopy (SEM) images were taken using FEI, Nova600 FEG-SEM model with acceleration voltage of 12 kV. The average particle size was determined by using ImageJ software. SEM samples were prepared by soaking the ITO slides in the iodine-activated AuSG MPCs solutions for 15 minutes, dried with N_2, and then the conductive side of the ITO slides were imaged for size analyses.

X-ray photoelectron spectroscopy (XPS) measurements. X-ray photoelectron spectroscopy (XPS) analyses were performed using a VG Scientific MultiLab 3000 ultra-high vacuum surface analysis system that is equipped with a dual-anode (Mg/Al) X-ray source and a CLAM4 hemispherical electron energy analyzer. The measurements were conducted using non-monochromatized Al K_α X-ray radiation ($h\nu \approx 1486.6$ eV) as the X-ray source and at a base pressure in the 10^{-9} Torr range. XPS spectra were collected at an electron emission angle of 54.7° relative to the surface normal. Aqueous solutions (200 μL) of AuSG (4 mg/mL) and PdSG (3 mg/mL) were drop-cast deposited on top of black carbon tape and air-dried for 2 hours before loading. Survey spectra were recorded between 50-450 eV BE for N, S, Pd and Au and between 610-640 eV BE for I.

Thermogravimetric analysis. Material compositions of the synthesized AuSG and PdSG MPCs were determined by measuring the weight changes using a TA Instruments thermogravimetric analyzer, model TA 2050, under a nitrogen atmosphere from 25 °C to 800 °C with a heating rate of 5 °C min^{-1} for AuSG MPCs and from 25 °C to 600 °C with a heating rate of 5 °C min^{-1} for PdSG MPCs. TGA also was used to determine the change in the % weight loss

upon treatment of PdSG MPCs with different equivalents of I_2. For this study, the MPCs were prepared as follows: PdSG MPCs (20.5 mg) were dissolved in nanopure water (2 mL) followed by addition of varying equivalents of I_2 (e.g., 24 μL of a 20 mM methanolic I_2 solution for addition of 0.025 eq). The mixture was reacted at room temperature for 3 hours, whereupon the MPCs were precipitated by addition of THF (2 mL) followed by sedimentation via centrifugation (4000 rpm, 10 min). The supernatant was removed and fresh THF (2 mL) was added to rinse the MPCs followed by centrifugation. The MPCs were rinsed using this process one additional time for complete removal of disulfide species prior to analysis by TGA.

UV-Vis Spectroscopy measurements. UV–Vis spectra were recorded on a Varian UV-Visible spectrophotometer, model CARY 50 Bio. All spectra were scanned from 300 nm to 800 nm at a fast scan rate using aqueous solutions of AuSG MPCs in a quartz cuvette. The background was subtracted using nanopure H_2O as the blank. First, AuSG MPCs (2.1 mg) were dissolved in nanopure H_2O (20 mL). Then, 1.5 mL of this stock solution was added to a cuvette and diluted to 3.0 mL final volume (diluted with H_2O and/or methanolic I_2 solutions) for the UV-Vis recordings. Based on the TGA data (33% organic composition, 1.7 x 10^{-4} mmol thiolates), 1.43 mM methanolic I_2 solution was prepared, and 30 μL to 240 μL of the prepared solution was added to the cuvette to afford 0.25 eq to 2.0 eq I_2:SG ratios, respectively. For PdSG MPCs, a 10 μL aliquot of the aqueous layer was diluted to 3 mL using nanopure water for analysis as a function of reaction cycles.

^{1}H NMR measurements. ^{1}H NMR spectra were recorded on a Varian 400 MHz spectrometer using D_2O as the solvent. AuSG MPCs (40 mg) or PdSG MPCs (40 mg) were dissolved in 450 μL D_2O and the resultant solution was added to an NMR tube. To the MPCs solution in the NMR tube was added a solution of *t*-butanol (internal standard) in D_2O (50 μL of a 0.38M

solution, 0.019 mmol). Deuterated methanol (100 μL) containing different amounts of I_2 was added to the MPCs solution and the mixtures were allowed to react for 40 minutes before measuring spectra. For example, the NMR tube reaction of AuSG MPCs with 0.25 eq I_2 contained 40 mg of AuSG MPCs in 450 μL D_2O, 50 μL of a 0.38 M *t*-butanol solution in D_2O, and 100 μL of a 0.106 M I_2 solution in CD_3OD (0.0106 mmol).

Gas chromatography measurements. The progress of the PdSG MPCs catalyzed reaction was monitored by gas chromatography (GC). The GC data was recorded on a Buck Scientific model 910 GC equipped with a 1/8th inch packed column (10% Carbowax 20M on silica 80/100 mesh, 6 foot) using a flame ionization detector (FID) and helium as the carrier gas. The method developed for GC includes injecting 1 μL of sample solution and using a temperature gradient for elution: hold at 80 °C for 2 min, ramp at 25 °C/min to 135 °C and then hold for 1 min. The pressure was varied from a start of 12 psi helium, holding for 3 min, to 14 psi helium for 2 min.

Results and Discussion

Characterization of AuSG MPCs and PdSG MPCs. TGA analysis of AuSG MPCs indicated a composition of ~33% organic and 67% Au metal (see Supporting Information, Figure S1A). The UV-Vis absorbance of the synthesized MPCs did not show the presence of a plasmon band (Figure S2A) suggesting that the synthesized particles have diameters <2 nm.[34] TEM analysis of the AuSG MPCs show roughly spherical particles with an average diameter of 1.6 ± 0.3 nm (Figure 1A, size histogram shown in Figure S3A). TGA analysis of the PdSG MPCs indicated an organic composition of 29% (Figure S1B) and in agreement with prior observations,[35] the UV-Vis absorbance of the PdSG MPCs did not show a plasmon band (Figure S2B). The TEM analysis showed an average particle diameter of 2.6 ± 0.5 nm (Figure 1B, size histogram shown

in Figure S3B), which is similar to the core diameter previously reported for glutathione-protected PdSG MPCs synthesized under these conditions.[14] ^{1}H NMR analyses of the Au and Pd MPCs confirmed attachment of glutathione. The appearance of well-broadened glutathione peaks in the ^{1}H NMR spectrum and specifically the disappearance of the methylene protons adjacent to the glutathione thiol group at δ ~2.95 ppm provide evidence that the synthesized MPCs are glutathione-protected.

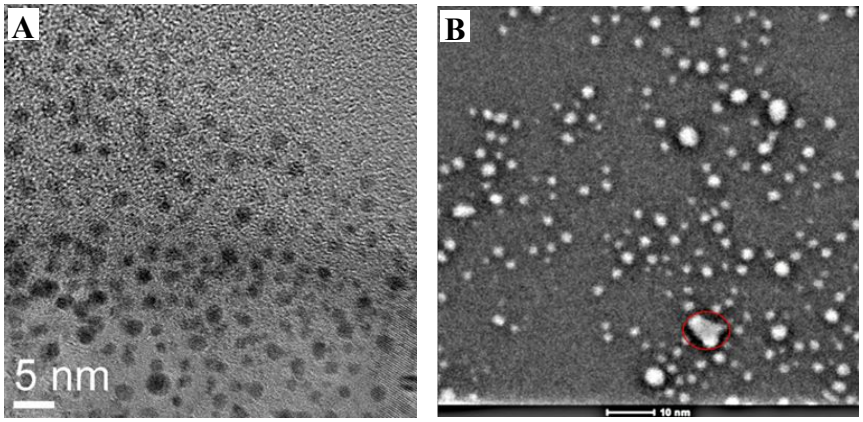

Figure 1. Characterization of synthesized MPCs. **A**: Brightfield TEM image of AuSG MPCs, and **B**: Darkfield TEM image of PdSG MPCs (red, circled aggregated sphere was not counted in the size analysis)

Catalytic reduction of 4-nitrophenol. The reduction of 4-nitrophenol (4-NP) using $NaBH_4$ (Scheme 2) proceeds slowly without addition of AuSG MPCs, requiring up to two days for completion.[36, 37] The reaction is conveniently followed using UV-Vis absorption spectroscopy by monitoring the disappearance of 4-nitrophenolate at 400 nm and the appearance of 4-aminophenolate (4-AP) at 300 nm (Figure S4). In the presence of a catalytic amount of an Au MPC catalyst, however, product formation ensues rapidly (Figure 2A). The addition of catalytic AuSG MPCs resulted in complete reduction of 4-NP within 40 minutes (rate constant of 0.066 min^{-1}). The catalytic activity has been attributed to a rate enhancement derived from association

of both $NaBH_4$ and 4-NP at the surface of the Au MPCs.[29] Specifically, the reaction rate is related to the total metal surface atoms available for the reduction of adsorbed 4-NP by a surface-hydrogen species formed on reversible transfer of hydride by adsorbed $NaBH_4$.[38] With this in mind, we turned our attention to increasing the accessibility of the reactants to the metal surface.

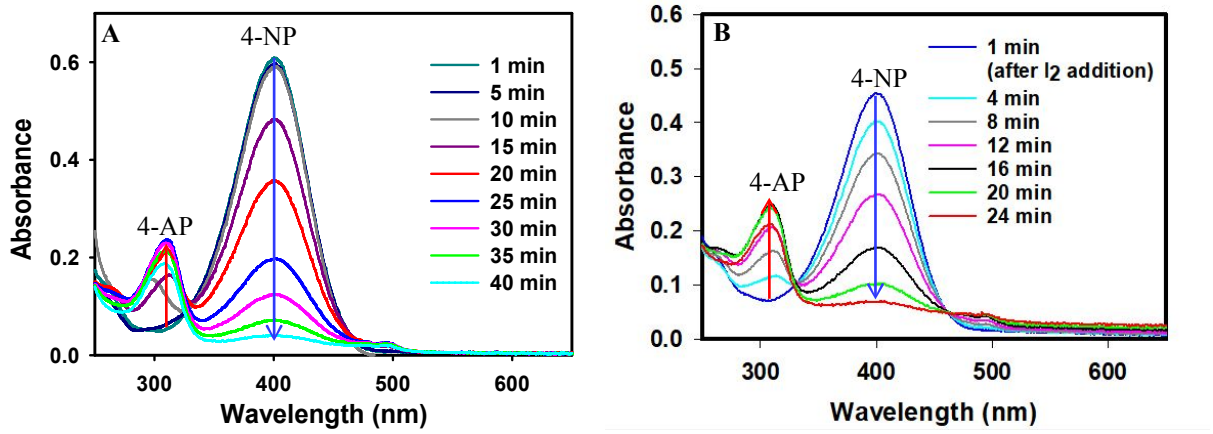

Figure 2. **A**: changes in absorbance during $NaBH_4$ reduction of 4-NP in the presence of AuSG MPCs as a catalyst over 5-minute intervals (no I_2 added). **B**: changes in absorbance during the AuSG MPC-catalyzed $NaBH_4$ reduction of 4-NP with 0.25 equivalents of I_2 addition.

Iodine activation of AuSG MPCs. The addition of I_2 to the reduction mixture containing AuSG MPCs dramatically increased the reaction rate. In comparison to the rate of reaction in the absence of added I_2, addition of I_2 at a 0.25 I_2:SG ratio enhanced the catalytic activity of the AuSG MPCs to completely reduce the 4-NP within 24 minutes (Figure 2B), as shown by the plot of $\ln(\text{absorbance}_{\text{initial}}\ (A_o)/\text{absorbance}_{\text{time}}\ (A_t))$ for the reaction (Figure 3A). Here, A_o refers to the initial absorbance that was taken at the beginning of the reaction and A_t refers to the absorbance at particular time. The reaction was modeled using pseudo first-order kinetics to determine the rate constant for the catalytic activity as reported previously.[39] Addition of more I_2 resulted in even faster reduction rates — the addition of 2.0 equivalents of I_2 resulted in complete reduction within 4 minutes. A control experiment in which I_2 was added (I_2:SG ratio = 2.0) to a mixture of

4-NP and $NaBH_4$ in the absence of AuSG MPCs showed that I_2 addition by itself did not affect the reaction rate. The rate constant for the AuSG MPC-catalyzed reaction in the absence of I_2 was 0.066 min^{-1} (Figure 3B), which is faster than a reported rate constant of 0.00005 min^{-1} observed for the 4-NP reduction catalyzed by DMF-stabilized AuSG MPCs.[40] The coordinating effect of DMF in this case[41] may be responsible for the slower reaction rate. In the present case, as more I_2 was added, the reaction rate continued to increase, reaching a nearly 8-fold enhancement to 0.505 min^{-1} for a ratio of 2.0 I_2:SG.

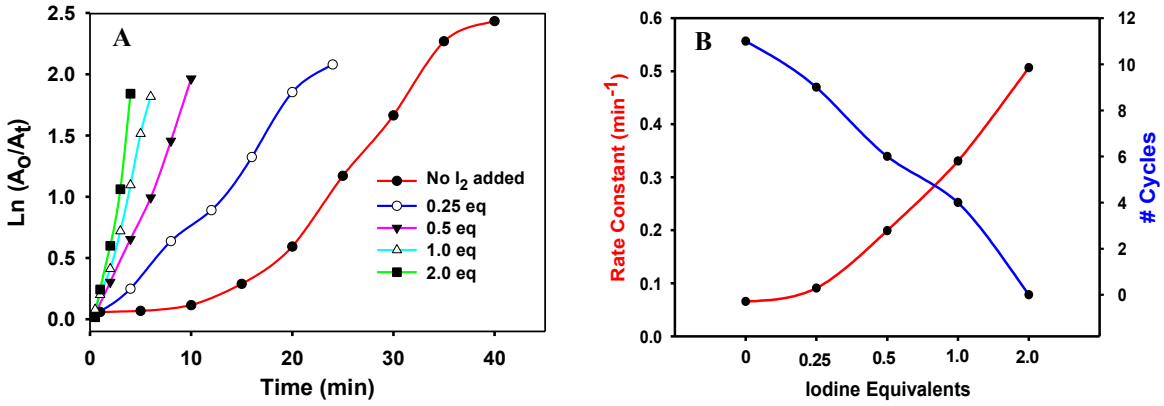

Figure 3. **A**: Plots of $ln(A_o/A_t)$ vs. time for the AuSG MPC-catalyzed reduction of 4-NP with different amounts of added I_2; **B**: plot of reaction rate constants (left y-axis, red) calculated from Fig. 3A and correlation with recyclability (right y-axis, blue).

Recyclability of AuSG MPCs. While I_2 addition enhanced the catalytic activity, the I_2 negatively affected the AuSG MPCs as evidenced by the reduced recyclability (Figure 3B). The untreated AuSG MPCs showed the ability to reduce 4-NP to completion in eleven consecutive reduction cycles at a gradually decreasing reaction rate for each subsequent cycle (Figure 4A). In contrast, when an I_2 ratio of 2.0 eq was added to the catalyst, no reactivity occurred on the second cycle, likely due to complete removal of SG ligands followed by Au core aggregation and

dissolution (Figure S5). The addition of 0.25 equivalents, however, showed comparable recyclability to the AuSG MPCs without I_2 while significantly enhancing the catalytic activity.

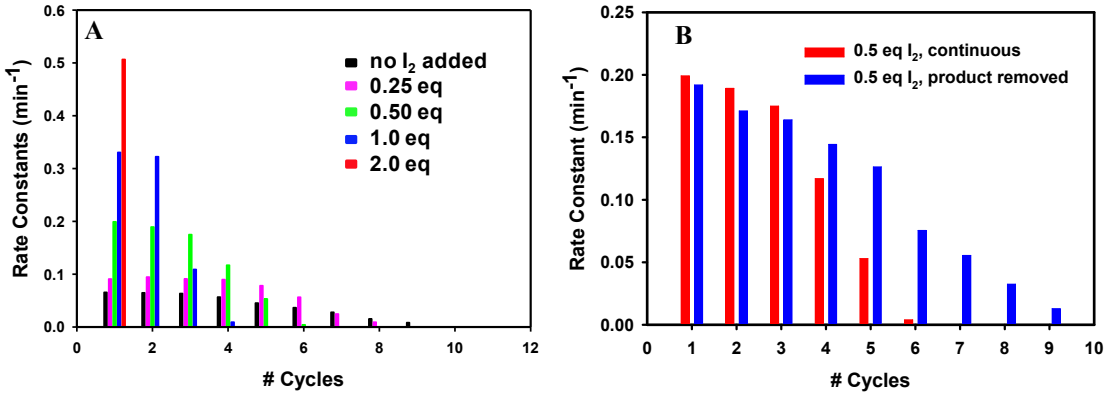

Figure 4. **A**: Plot of rate constant values vs. recyclability for 4-NP reduction with varying equivalents of added I_2; **B**: plot of rate constant values vs. number of cycles for the reduction with 0.5 equivalents of added I_2, with and without products removed in subsequent cycles.

To further explore the recyclability of I_2-activated AuSG MPCs, a large-scale reaction was performed in which THF was added to the reaction mixture after each cycle to precipitate the AuSG MPCs for isolation via centrifugation and to remove the 4-AP product by separation of the THF supernatant. The collected MPCs were then used to catalyze another reaction cycle. This experiment was designed to study the effect of 4-AP on catalyst recyclability. We hypothesized that the build-up in concentration of 4-AP, formed with each consecutive cycle, might hinder AuSG MPC activity. If this is true, then removing the product at the end of each cycle should increase the number of active catalytic cycles. Figure 4B shows a comparison between the catalytic activity observed when 0.5 eq of I_2 were added and the product was allowed to amass continuously upon each reaction cycle vs. the experiment in which the product was removed by precipitation and centrifugation with each cycle. The catalyst was active for 9 cycles when

removing the product after each cycle as compared to being active for 5 cycles when the product was allowed to accumulate in solution.

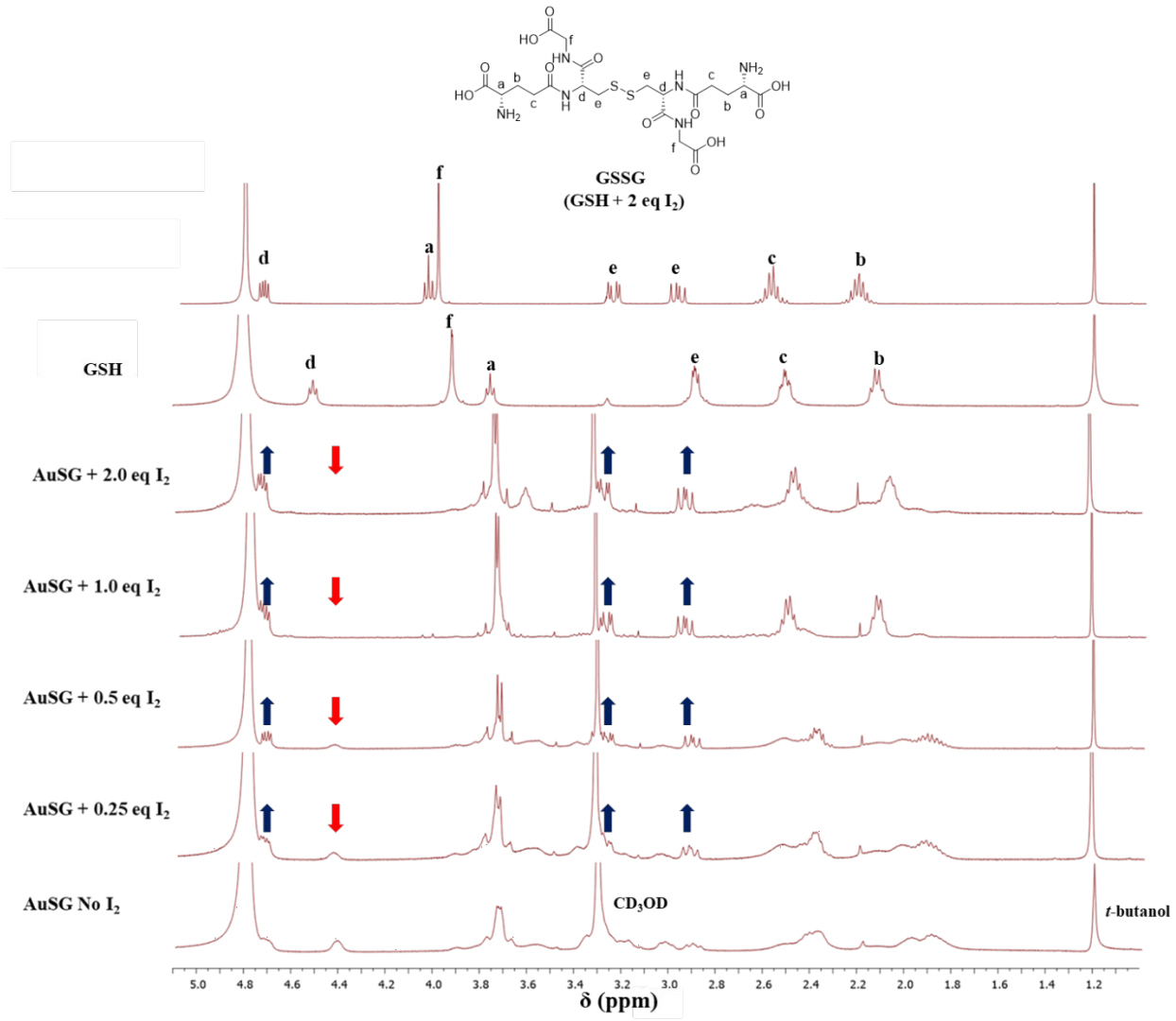

Figure 5. ^{1}H NMR spectra of AuSG MPCs in D_2O without added I_2 and 40 min after the addition of various equivalents of I_2. The signals at δ2.93-2.99 and 3.27-3.32 ppm (marked by blue arrows) correspond to the methylene protons of the cysteine residues of glutathione disulfide (GS-SG), and the signal at δ4.72-4.76 ppm corresponds to the adjacent methine proton (far left blue arrow). The increase in these signals on addition of I_2, relative to the internal standard *t*-butanol singlet at δ1.19 ppm, indicates that the disulfide forms and dissociates from the AuSG MPCs. With no I_2, the methylene protons next to S of bound glutathione are not visible in the NMR spectrum and the signal for the immediately adjacent methine proton appears at δ4.44 ppm (red arrow) as a broad peak, indicating that the SG is bound to the Au cluster. The

peak height decreases with added I_2 in agreement with ligand removal upon disulfide formation. The NMR spectra of free glutathione (GSH) and GSH oxidized to disulfide by I_2 are shown for comparison. Some differences in chemical shifts for the signals of GS-SG formed on reaction of AuSG MPCs vs. I_2-oxidation of free GSH can be expected, particularly for protons adjacent to N groups, due to differences in pH and the presence of metal ions.

NMR Studies of I_2 Addition to AuSG MPCs. The rate enhancement data are consistent with the assertion that I_2 functions to remove glutathione ligands from the surface of the AuSG MPCs as disulfides (GS-SG) to provide better access of the reactants to the Au surface, which in turn enhances the catalytic activity. To confirm this and quantify the amount of SG ligand removal, we added varying equivalents of I_2 to AuSG MPCs in D_2O relative to the SG ligands and analyzed the amount of dissociated GS-SG by ^{1}H NMR spectroscopy after 40 min of reaction (Figure 5). The addition of I_2 removed a proportionate amount of bound glutathione from the surface of the Au core, as evidenced by the appearance of signals corresponding to CH_2 protons next to the disulfide group at δ2.93-2.99 and 3.27-3.32 ppm (blue arrows) in the ^{1}H NMR spectra. As the amount of I_2 increased, the area of these signals increased. We also observed a decrease in the signal of the CH proton of the -C*H*CH_2S-Au of bound glutathione at δ4.44 ppm (red arrow), indicating ligand removal from the MPCs in correlation with added I_2. We quantified the signal at δ2.93-2.99 ppm as a function of added I_2 by comparing it to the intensity of the *t*-butanol internal standard signal at δ1.19 ppm. Assuming 100% of the SG ligands were removed as GS-SG at 2.0 eq I_2, we calculated that 37% of the SG ligands were removed from AuSG MPCs on addition of 0.125 eq I_2, 53% on addition of 0.25 eq, 83% on addition of 0.50 eq, and 97% on addition of 1.0 eq I_2 (see Table 1). These calculations in combination with the rate data show that 37% ligand removal does not significantly enhance the catalytic activity, while 53% ligand removal shows enhanced activity with high recyclability. 83% ligand removal is close to optimal in terms of high rate enhancement while maintaining recyclability. Beyond that,

any benefit from rate enhancement is negated by very poor recyclability due to catalyst instability.

Table 1. Quantitative results from the NMR data (Figure 5) showing the percent of ligand removal from AuSG MPCs as a function of added I_2 equivalents after 40 min. reaction.

I_2 equivalents	Ratio of Disulfide/*t*-butanol Integration	Ratio/Ratio at 2 equiv.	% Ligand Removal
0	0	0/0.57	0
0.125	0.21	0.21/0.57	36.8
0.25	0.3	0.30/0.57	52.6
0.5	0.47	0.47/0.57	82.5
1.0	0.55	0.55/0.57	96.5
2.0	0.57	0.57/0.57	100

UV-Vis Study of AuSG MPC Stability. We measured the absorbance spectra of aqueous solutions of AuSG MPCs treated with different equivalents of I_2 and monitored their stability from 30 s to 3 h (Figure S5). In agreement with recyclability trends and noticeable changes in the MPCs with increasing I_2 equivalents, the UV-vis spectra of the AuSG MPCs showed the development of a localized surface plasmon resonance (LSPR) peak for Au at ~530 nm with 0.50 and 1.0 eq of I_2 added (Figure S5B and S5C). This indicates enlargement of the Au MPCs by aggregation or ripening. The addition of 0.25 equivalents of I_2 did not lead to any significant changes in the UV-vis spectra, indicating no growth or aggregation of the MPCs, consistent with their higher stability/recyclability (Figure S5A). The addition of excess I_2 (2.0 eq) resulted in a large decreas in absorbance and the appearance of two absorbance peaks at 352 nm and 454 nm, indicative of dissolution of the Au to form soluble Au^{I} or Au^{III} iodide ionic complexes (Figure S5D). The kinetics of gold dissolution in the presence of iodide has been previously reported.[42] Furthermore, these observations are consistent with the changes we noted in the solution color of the AuSG MPCs (Figure S5 Top).

Iodine-activated AuSG MPCs characterized by scanning electron microscopy (SEM) agree with the UV-vis data. At an I_2:SG ratio of 0.25, no change in particle size was observed based on the MPCs being difficult to observe by the SEM since 1.6 nm is below our resolution (Figure S6A). At an I_2:SG ratio of 0.5, the SEM images showed nanoparticles with an average diameter of 68 ± 7 nm, indicative of MPCs growth into larger nanoparticles (Figure S6B). At an I_2:SG ratio of 1.0, the average diameter of the nanoparticles increased to 497 ± 33 nm (Figure S6C), consistent with the larger LSPR band in Figure S5C. In agreement with the observed dissolution of Au, no particles were observed at an I_2:SG ratio of 2.

Catalytic hydrogenation/isomerization of allyl alcohol. The catalysis of allyl alcohol hydrogenation/isomerization (Scheme 2) to 1-propanol (hydrogenation product) and propanal (isomerization product) using alkanethiolate-capped Pd nanoclusters is well understood.[4,15] We

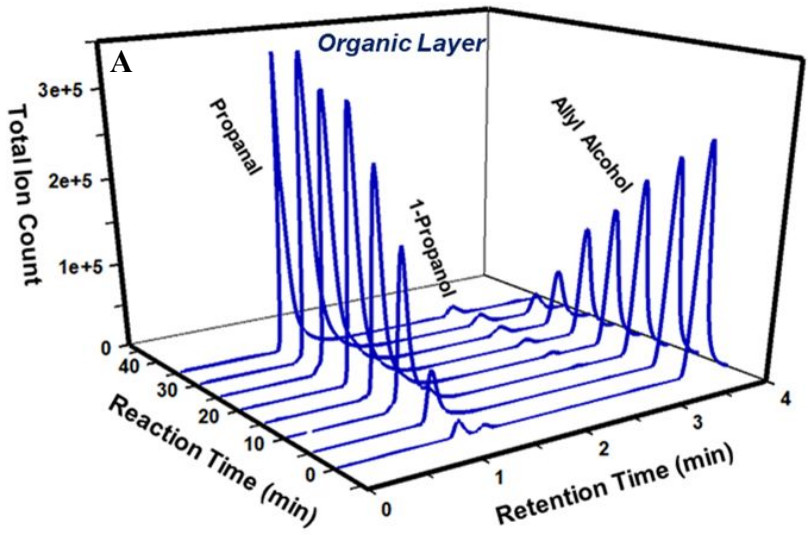

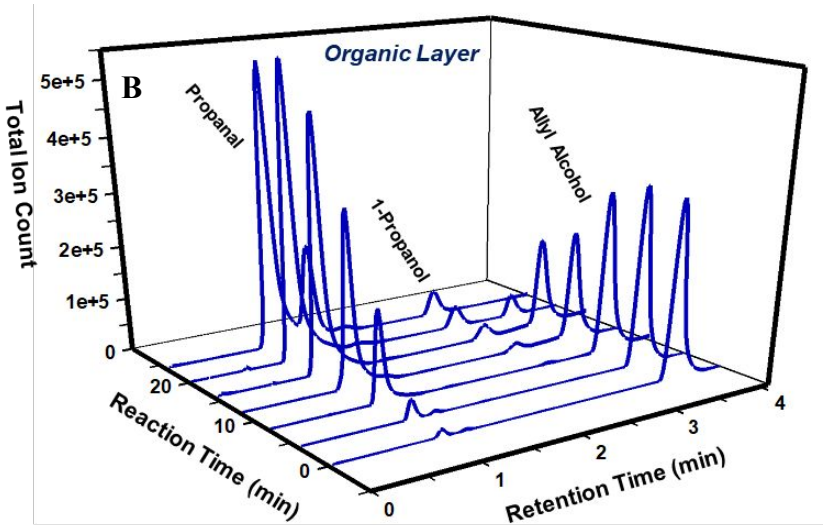

Figure 6. GC-FID chromatograms of allyl alcohol hydrogenation/ isomerization using PdSG MPCs in chlorobenzene:water (1:1) with a H_2 flow rate of 20.0 ± 0.5 mL/min. **A**: organic phase, in absence of I_2; **B**: organic phase, with 0.05 eq I_2 addition.

performed this reaction using PdSG MPCs in a chlorobenzene-water biphasic system while passing H_2 through the mixture using a glass pipette (Figure S7). Figure S8 shows the GC-FID chromatograms of allyl alcohol, propanal and 1-propanol (all 10 mM), indicating the retention times of each components in both organic and aqueous phase. The progress of the PdSG MPC-catalyzed reaction was monitored by examining both phases at 5-minute intervals using GC (organic phase, Figure 6A; aqueous phase, Figure S9A, No I_2 added). In both the organic and aqueous phases, the allyl alcohol (t_r =3.6 min) disappeared within 35 minutes, while peaks corresponding to propanal (t_r =1.1 min) and 1-propanol (t_r = 2.9 min) increased over time. The product distribution depended on the phase, as the isomerized product was more favored in the organic phase while a ~1:1 mixture of isomerized:hydrogenated products appeared in the aqueous phase (overall selectivity was 80-90% isomerized product). We next turned our attention to examining the effect of adding varying amounts of I_2 on the reaction rate and catalyst recyclability.

Iodine activation of PdSG MPCs. The addition of I_2 to the reaction mixture containing PdSG MPCs and allyl alcohol significantly increased the reaction rate. Figure 6B (organic phase) shows that the addition of 0.05 equivalents of I_2 enhanced the catalytic activity, as it only took 24 minutes in comparison to 35 minutes in the absence of I_2 for complete conversion (see Figure S9B for aqueous phase with 0.05 eq I_2). The total percentage completion plot shows that the reaction was completed nearly twice as fast when 0.2 equivalents of I_2 were added as compared to the reaction without I_2 (Figure S10). Catalytic enhancement is noted with addition of as little as 0.025 equivalents of I_2. TOF values were determined from the plots of the %hydrogenation and %isomerization vs reaction time and taking the slope of the plots with <60% corresponding conversions (Figure S11). Table 2 summarizes the turnover frequencies (TOFs) for the reaction in the absence and presence of varying equivalents of added I_2. The TOFs were calculated by measuring the response factor of 1-propanol and propanal relative to allyl alcohol from a GC of standard solutions of 10 mM each (Figure S8), which allowed a measurement of the percent of allyl alcohol converted to 1-propanol and propanal as a function of time according to a method reported in the literature (see page S-8 of Supporting Information).[43] The total TOF (hydrogenation TOF plus isomerization TOF) significantly increased from 131 to 230 moles products/moles Pd/h on increasing the I_2:SG ratio from 0.025 to 0.2. However, at a ratio higher than 0.3, there was little conversion of allyl alcohol into products, even after 60 minutes of reaction time.

Recyclability of PdSG MPCs. In that we used a biphasic system for the reaction, the PdSG MPCs were readily isolated from the aqueous phase for use in subsequent cycles. For each subsequent reaction, fresh allyl alcohol was added to determine the recyclability of the catalyst. We observed that the catalyst could be recycled up to 4 times in the absence of I_2 (Table 2 and

Table 2. Turnover frequency and catalyst recyclability for the PdSG MPCs-catalyzed hydrogenation/isomerization of allyl alcohol with and without added I_2. TOFs are determined from the slopes of the plots at <60% allyl alcohol conversion to products.

	No I_2 added	**Equivalents of added I_2**				
		0.025	**0.05**	**0.1**	**0.2**	**0.3**
Hydrogenation TOF[a]	12	17	22	26	28	<5% converted
Isomerization TOF	119	144	172	197	202	<5% converted
Total TOF	131	161	194	223	230	-
Hydrogenation %[b]	9	11	11	12	12	-
Isomerization %[c]	91	89	89	88	88	-
Recyclability[d]	4	4	3	2	1	-

[a]TOF given in moles product/moles Pd/h (combined aqueous and organic phase); [b]percentage of 1-propanol formed; [c]percentage of propanal formed; [d]number of cycles after initial reaction that the isolated catalyst completely transformed allyl alcohol into products within 60 minutes.

Figure 7). Importantly, the addition of 0.025 eq I_2 maintained higher TOFs in each subsequent cycle relative to the reaction without added I_2, without affecting the recyclability of the catalyst. However, addition of greater amounts of I_2 degraded the recyclability of the catalyst, presumably a consequence of particle aggregation, growth, and possibly even dissolution caused by I_2. GC-FID chromatograms of 5 different cycles (recyclability = 4) of allyl alcohol hydrogenation/ isomerization in the absence of I_2 are shown in Figure S12. Although the particles were stable during their first cycle (Figure S13A), the UV-Vis spectra of PdSG MPCs show evidence of aggregation at the stage of the last cycle, as noted in Table 2, for all conditions (Figure S13B). Aggregation of the MPCs treated with 0.2 eq I_2 was the most pronounced, consistent with the activity being limited to only one catalytic cycle (Table 2). Reactions attempted with even higher amounts of added I_2, such as 0.3 eq and 0.6 eq, did not result in any product formation, suggesting even more severe instability due to aggregation or dissolution of the PdSG MPCs.

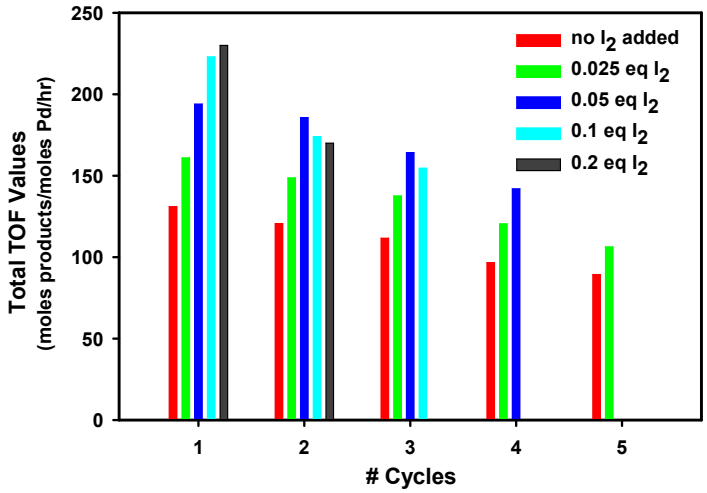

Figure 7. Plot of total TOF values vs. number of reaction cycles for hydrogenation/ isomerization of allyl alcohol using catalytic PdSG MPCs with and without added I_2. Successful cycle completion required that 100% of allyl alcohol be transformed into products within 60 minutes.

NMR Studies of I_2 Addition on PdSG MPCs. The activity for hydrogenation/isomerization increases with increasing I_2 added, but the number of equivalents needed for activity and MPC stability was much lower than that observed for AuSG MPCs. This led to questions about whether the activation mechanism was the same for AuSG and PdSG MPCs. The smaller equivalents of I_2 needed for enhanced catalytic activity of PdSG compared to AuSG MPCs may be related to the iodide-catalyzed oxidation of Pd, as reported by Soriaga and co-workers.[44] Also, studies conducted by Biffis and co-workers suggested that Pd^{II} species leach into solution during a cross-coupling reaction, where they catalyze the reaction and may form the cluster again.[45] Shon and co-workers examined the leaching of Pd^{II} from octanethiolate Pd MPCs during a catalytic cycle by ICP-OES and found up to ~0.05 ppm Pd^{II} in the solution.[46] We conducted NMR studies on the addition of 0.05 to 0.6 eq of I_2 to PdSG MPCs in D_2O using a *t*-butanol internal standard as described for AuSG MPCs NMR study (Figure S14). Surprisingly, while we

found that some signals in the NMR spectra sharpened with increasing amounts of I_2, indicating removal of SG ligands from the MPCs, we did not observe the characteristic GS-SG signals at δ2.93-2.99, 3.27-2.32, and 4.72-4.76 ppm corresponding to disulfide formation. This suggests that the SG ligands dissociate from the PdSG MPCs in another form, possibly as Pd(II)-SG complexes (oligomers, clusters, or polymers), which might be expected to produce poorly resolved signals. In fact, NMR spectra of $Pd^{II}Cl_4^{2-}$ intentionally added to GSH and GSH plus I_2 also did not show well-resolved peaks that are characteristic of GS-SG formation (Figure S15). This is also consistent with previous observations of Pd(II) leaching and the strong ability of iodide to catalyze Pd oxidation compared to Au. With small amounts of added I_2, we believe that small amounts of Pd(II)-SG species dissociate from the PdSG MPCs to expose bare Pd sites for enhanced catalytic activity. While this mode of catalyst activation is not conclusive, it is clear that SG ligands somehow dissociate from the PdSG MPCs in a manner that does not lead to detectable GS-SG or GSH. Without disulfide formation, it was difficult to quantify ligand loss by NMR. Using TGA, however, we measured the % organic composition after treatment with various amounts of I_2, which revealed that the organic weight decreased by 5 to 38% for 0.025 to 0.2 eq of I_2 added, respectively (Figure S16). This confirms that ligand loss did occur.

Activation of AuSG and PdSG MPCs. Our data is consistent with two different I_2 activation mechanisms for AuSG and PdSG MPCs. With Au, the NMR data very clearly show ligand dissociation by disulfide formation as shown in Scheme 1. Small amounts of I_2 decrease the ligand density while the Au MPCs remain stable. Larger amounts of I_2 lead to destabilization of the Au MPCs through aggregation and even complete dissolution of Au with the largest amounts of I_2 studied (2.0 eq) over longer times. Optimal ligand removal for improved catalytic rates and

good recyclability is in the 50-80% removal range. For PdSG MPCs, the I_2 also removes SG ligands, but in a very different way not consistent with Scheme 1. First, ligand removal ranged from 5 to 38% for much smaller amounts of added I_2. Second, the ligands are not removed as disulfides. While not conclusive, the data suggests that Pd oxidation occurs and the ligands are removed as Pd(II)-thiolate species. There may also be Pd(II) iodide complexes formed. Pd oxidation is likely an issue since adding 0.3 and 0.6 I_2 eq, which work fine for Au, does not result in any catalytic activity for Pd. This shows major changes in the Pd MPCs likely associated with Pd aggregation, oxidation, and dissolution.

An interesting question in both systems concerns the fate of the I_2/I^- species. I_2 becomes reduced to $2I^-$ during sulfide formation or metal oxidation. The XPS data obtained on AuSG and PdSG MPCs after treatment with various eq I_2 under catalytic reaction conditions show that I^- adsorbs to the Au and Pd surfaces (Figure S17A and S17B, respectively). The signal was weak in some cases and we were not able to quantify it reliably, making the extent of I^- coverage difficult to confirm. We can confidently say that a measurable amount of I^- adsorbs to both Au and Pd, however. While I^- may still inhibit active sites on the Au and Pd surfaces, it is apparently not as poisoning as the original glutathione ligands, so increased reactivity still occurs. It is also likely for some I^- to dissolve into solution or form Au(I)/Au(III) iodide or Pd(II) iodide ionic complexes, based on the evidence of metal dissolution. Despite some evidence of metal dissolution, the metallic ions are not the active catalysts, since deactivation is associated with larger amounts of I_2. XPS spectra of the Au region shows primarily Au(0) while the Pd shows a mixture of Pd and Pd(II) species (Figure S18). More work will be required in the future to better understand the full details of the MPC activation mechanism and catalyst activation site.

Conclusions

Using two organic reactions as representative models, our results demonstrate that the catalytic activity of thiolate-protected metal nanoclusters can be increased by the addition of trace levels of iodine. The improvement in catalytic activity likely is the result of decreased ligand surface density that occurs on I_2 addition. The method is straightforward relative to other ligand removal strategies used to expose metal cores and enhance metal-substrate interactions. The analytical techniques that we employed (^{1}H NMR, TGA, UV-Vis, XPS, and SEM) to characterize AuSG and PdSG MPCs before and after addition of I_2 collectively indicate that the I_2 functions to promote ligand dissociation through disulfide formation in the case of Au and through Pd(II)-thiolate formation in the case of Pd.[25] Both the catalyzed reduction of 4-nitrophenol by AuSG MPCs and hydrogenation/isomerization of allyl alcohol by PdSG MPCs were accelerated by addition of I_2 (7-fold and 2-fold rate enhancement for Au and Pd, respectively). A judicious choice in the amount of added I_2, however, is required to prevent particle (catalyst) instability, an important consideration for catalyst recyclability. In both cases examined, a threshold was observed for I_2-induced removal of too many surface thiolates resulting in catalyst deactivation due to aggregation, precipitation, and even dissolution. Thiolate-protected metal cluster immobilization on solid supports may circumvent problems associated with particle aggregation, yet still allow catalytic enhancements afforded by exposure to I_2.[47] The present strategy also may find utility in amplifying responses of thiolate monolayer-protected metal-based chemiresistors, where electron transport properties are ligand-dependent. Whereas these applications remain to be studied, the applicability of this general approach for thiolate ligand

removal from homogeneous metal MPC catalysis is promising based on the results presented herein.

Supporting information

The supporting information is available, characterization of synthesized clusters includes TGA, UV-vis, TEM, SEM, ^{1}H NMR, UV-VIS, XPS, and GC data (14 pages).

Conflicts of Interest

The authors declare no conflict of interest.

Acknowledgements

This work was supported by NIH (P42 ES023716) and the National Science Foundation (CHE-1611170).

References and notes

1. M. D. Hughes, Y. J. Xu, P. Jenkins, P. McMorn, P. Landon, D. I. Enache, A. F. Carley, G. A. Attard, G. J. Hutchings, F. King, E. H. Stitt, P. Johnston, K. Griffin and C. J. Kiely, *Nature,* 2005, **437**, 1132–1135.
2. G. Li and R. Jin, *Acc. Chem. Res.,* 2013, **46**, 1749–1758.
3. M. Dasog, W. Hou and R. W. J. Scott, *Chem. Commun.,* 2011, **47**, 8569–8571.
4. D. J. Gavia and Y.-S. Shon, *Langmuir,* 2012, **28**, 14502–14508.
5. K. A. San, V. Chen and Y.-S. Shon, *ACS Appl. Mater. Interfaces,* 2017, **9**, 9823-9832.
6. P. Wand, E. Kratzer, U. Heiz, M. Cokoja and M. Tschurl, *Catalysis Communications,* 2017, **100**, 85-88.
7. F. Lu, J. Ruiz and A. Didier, *Tetrahedron Lett.,* 2004, **45**, 9443-9445.
8. Y. Lu and W. Chen, *Chem. Soc. Rev.,* 2012, **41**, 3594-3623.
9. J. F. Parker, C. A. Fields-Zinna and R. W. Murray, *Acc. Chem. Res.,* 2010, **43**, 1289– 1296.
10. X. Kang, H. Chong and M. Zhu, *Nanoscale,* 2018, **10**, 10758–10834.
11. L. M. Rossi, J. L. Fiorio, M. A. S. Gracia and C. P. Ferraz, *Dalton Trans.,* 2018, **47**, 5889-5915.
12. S. E. Lohse, J. A. Dahl and J. E. Hutchison, *Langmuir,* 2010, **26**, 7504–7511.
13. Y. Ju-Nam, W. Abdussalam-Mohammed and J. J. Ojeda, *Faraday Discuss.,* 2016, **186**, 77–93.
14. S. Sharma, B. Kim and D. Lee, *Langmuir,* 2012, **28**, 15958–15965.
15. S. Bhama, T. R. Sibakoti, J. B. Jasinski and F. P. Zamborini, *Chem. Cat. Chem*., 2020, **12**, 1-10.

16. L. Lu, B. Lou, S. Zou, H. Kobayashi, J. Liu, L. Xiao and J. Fan, *ACS Catal.,* 2018, **8**, 8484–8492.
17. E. W. Elliott III, R. D. Glover and J. E. Hutchison, *ACS Nano,* 2015, **9**, 3050–3059.
18. Z. Niu and Y. Li, *Chem. Mater.,* 2014, **26**, 72– 83.
19. S. Brimaud, C. Coutanceau, E. Garnier, J. M. Léger, F. Gerard, S. Pronier and M. Leoni, *J. Electroanal. Chem*., 2007, **602**, 226−236.
20. G. Collins, F. Davitt, C. O'Dyer and J. D. Holmes, *ACS Appl. Nano Mater.,* 2018, **1**, 7129–7138.
21. D. A. Henckel, O. Lenz and B. M. Cossairt, *ACS Catal.,* 2017, **7**, 2815−2820.
22. T. R. Sibakoti, C. R. Stinger, P. K. Adhihetty, F. P. Zamborini and M. H. Nantz, *Part. Part. Syst. Charact.,* 2019, **36**, 1900093.
23. Z. Xie, M. V. R. Raju, A. C. Stewart, M. H. Nantz and X.-A. Fu, *RSC Advances*, 2018, **8**, 35618–35624.
24. M. Moreno, L. N. Kissell, J. B. Jasinski and F. P. Zamborini, *ACS Catal.,* 2012, **2**, 2602–2613.
25. A. C. Templeton, M. J. Hostetler, C. T. Kraft and R. W. Murray, *J. Am. Chem. Soc.,* 1998, **120**, 1906–1911.
26. L. Sun, R. M. Crooks and V. Chechik, *Chem. Commun.,* 2001, **4**, 359–360.
27. J. -B. Kim, M. L. Bruening and G. L. Baker, *J. Am. Chem. Soc.,* 2000, **122**, 7616–7617.
28. N. Pradhan, A. Pal and T. Pal, *Colloids and Surfaces A,* 2002, **196**, 247–257.
29. S. Wunder, F. Polzer, Y. Lu, Y. Mei and M. Ballauff, *J. Phys. Chem. C*, 2010, **114**, 8814–8820.
30. E. Sadeghmoghaddam, H. Gu and Y.-S. Shon, *ACS Catal*., 2012, **2**, 1838–1845.
31. K. Di Pietrantonio, F. Coccia, L. Tonucci, N. d'Alessandro and M. Bressan, *RSC Adv.,* 2015, **5**, 68493-68499.
32. B. P. Block, *Inorg. Synth.,* 1953, **4**, 14–17.
33. Z. Wu, J. Chen and R. Jin, *Adv. Funct. Mater.,* 2011, **21**, 177–183.
34. R. Jin, *Nanoscale*, 2010, **2**, 343.
35. E. Ringe, C. J. DeSantis, S. M. Collins, M. Duchamp, R. E. Dunin-Borkowski, S. E. Skrabalak and P. A. Midgley, *Sci Rep.,* 2015, **5**, 17431.
36. P. Herves, M. Perez-Lorenzo, L. M. Liz-Marzan, J. Dzubiella, Y. Lu and M. Ballauff, *Chem. Soc. Rev.,* 2012, **41**, 5577-5587.
37. K. K. Halder, S. Kundu and A. Patra, *ACS Appl. Mater. Interfaces,* 2014, **6**, 21946–21953.
38. P. Ngene, R. Van Den Berg, M. H. W. Verkukuijlen, K. P. De Jong and P. E. De Jongh, *Energy Environ. Sci.,* 2011, **4**, 4108–4115.
39. Z. V. Feng, J. L. Lyon, J. S. Croley, R. M. Crooks, D. A. Vanden Bout and K. J. Stevenson, *J. Chem. Educ.,* 2009, **86**, 368-372.
40. H. Yamamoto, H. Yano, H. Kouchi, Y. Obora, R. Arakawa and H. Kawasaki, *Nanoscale,* 2012, **4**, 4148–4154.
41. H. Yamamoto *et al.* (ref. 40) noted that the layer of adsorbed DMF prohibited the reactants from penetrating to the surface of the Au nanoclusters at the onset of the reaction, resulting in an induction time before 4-NP reduction could begin.
42. P. H. Qi and J. B. Hiskey, *Hydrometallurgy,* 1991, **27**, 47–62.
43. S. Bhattacharjee and M. Bruening, *Langmuir,* 2008, **24**, 2916–2920.

44. K. Sashikata, Y. Matsui, K. Itaya and M. P. Soriaga, *J. Phys. Chem.,* 1996, **100**, 20027-20034.
45. A. Biffis, M. Zecca and M. Basato. *Eur. J. Inorg. Chem.,* 2001, **2001**, 1131-1133.
46. T-A. Chen and Y-S. Shon. *Catal. Sci. Technol.,* 2017, **7**, 4823-4829.
47. J. A. Lopez-Sanchez, N. Dimitratos, C. Hammond, G. L. Brett, L. Kesavan, S. White, P. Miedziak, R. Tiruvalam, R. L. Jenkins, A. F. Carley, D. Knight, C. J. Kiely and G. J. Hutchings, *Nat. Chem.,* 2011, **3**, 551-556.

Table of Contents Graphic and Description

This work presents a general method of using iodine to partially remove thiolate ligands from metal clusters, resulting in significant catalytic enhancement.